Simultaneous Production of Freshwater and Energy from Saline Water using Hybrid Capacitive Deionization-Reverse Electrodialysis

Yusufu Abeid Chande Jande[1, 2] and Woo-Seung Kim[1,*]

***Abstract*—**Capacitive deionization (CDI) is an emerging desalination technology for purifying saline water. Upon the application of power ions from the saline water stream are adsorbed to the porous electrodes. Negative ions are attracted towards the positively biased electrode and the positive ions are attracted towards the negatively biased electrode. On the other hand, reverse electrodialysis (RED) is a power generating device by utilizing the salinity gradient. It contains permselective membranes in which only a certain ion species are allowed to pass through from the high salinity stream. In this study, the production of freshwater and energy using the hybrid CDI-RED system is presented. Saline water with a concentration of 15,000 ppm is initially fed to the CDI cell, which results in three streams: freshwater, lower salinity, and high salinity stream. The last two streams are fed to the RED to generate the average power density of around 0.26 W/m^2.

***Keywords*—** capacitive deionization, reverse electrodialysis, freshwater, power density.

I. Introduction

The availability of direct source of potable water is limited, thus alternative methods are sought. Through the use of desalination technologies freshwater can be acquired from seawater, underground water, or any brackish water sources [1-3]. The commonly used desalination technologies are reverse osmosis (RO), electrodialysis, ion-exchange resins, membrane distillation, multiflash distillation, vapor compression, multi-effect distillation, freeze desalination, and forward osmosis [4-6]. In recent years, other desalination technologies have been developed to determine their superiority, i.e., low energy consumption, than the conventional ones [7-9]. Among the emerging desalination technologies is capacitive deionization (CDI) [10].

The desalination via CDI cell involves the removal of ions from water the saline water stream. Initially the porous electrodes of the CDI cell are polarized using the applied DC power [11-14]. One of the electrodes becomes positively charged and the other one becomes negatively charged. When the salt rich water stream passes through the biased electrodes, negative ions are attracted towards the positive electrode and positive ions are attracted to the negative electrode. The adsorption of ions continues until the CDI cell is saturated with ions; thereupon desorption cycle begins after shorting the CDI cell (zero voltage application) or after reversing the polarity (applying reversed voltage). Fig.1 shows the schematic diagram of the half cycle of the CDI operation. The definition of cathode and anode in CDI is done during charging, whereas in traditional electrochemical cells (batteries) it is during discharging [15].

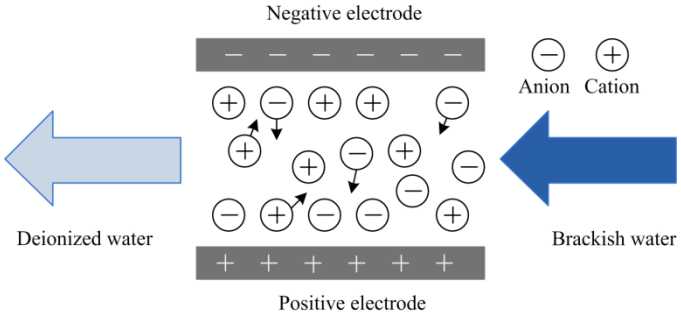

Fig. 1 Half cycle of CDI cell operation [11]

Apart from water shortages, energy crisis is one of the core world agenda. The fossil fuels are depleting at high rate leaving behind greenhouse gases[16, 17]. The use of alternative energy producing methods which are free from greenhouse gases is the ongoing research work worldwide. Reverse electrodialysis (RED) is among of alternative methods for generating electric power[18, 19]. In RED power is generated due to the salinity gradient between the high salinity stream (i.e., seawater) and low salinity stream (i.e., river water) (Fig. 2). As the membrane selectivity allows the ions to pass through, the voltage called Donnan potential develops. This power can be used to drive an electric device [20].

In this study we present the hybrid CDI-RED system in order to produce freshwater and at the same time generate electric power. The authors in references [21, 22] reported similar studies, but it involves the use of RO and RED. With the knowledge of the authors of this paper, there is no published paper reporting the integration of CDI and RED to produce freshwater and electricity simultaneously.

Yusufu Abeid Chande Jande[1,2] is with the Department of Mechanical Engineering, Hanyang University, 55 Hanyangdaehak-ro, Sangnok-gu, Ansan Kyeonggi-do 426-791, Republic of Korea and is with the Department of Materials Science and Engineering, Nelson Mandela African Institution of Science and Technology, Arusha, Tanzania (e-mail: yusufu.jande@nm-aist.ac.tz).

Woo-Seung Kim[1,*] is with the Department of Mechanical Engineering, Hanyang University, 55 Hanyangdaehak-ro, Sangnok-gu, Ansan Kyeonggi-do 426-791, Republic of Korea (Corresponding author: Tel.: +82 31 400 5248; fax: +82 31 418 0153 e-mail: wskim@hanyang.ac.kr).

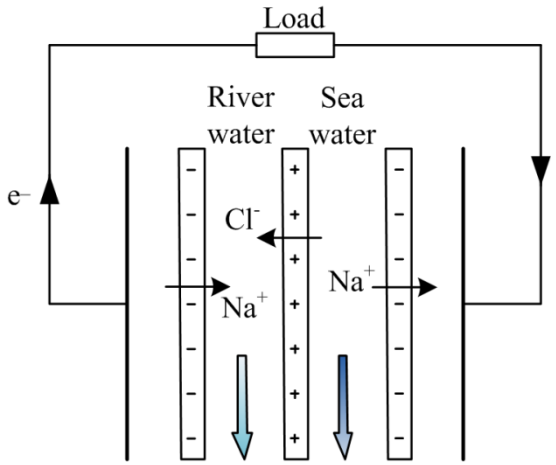

Fig. 2 Schematic diagram of reverse electrodialysis

II. METHODOLOGY

A. Capacitive Deionization

The model by Jande and Kim [23] is used to find out the CDI operating parameters such as capacitance, flow rate, spacer volume, dead volume, and resistance when the saline water with the concentration of 1500 ppm is fed. Note that in this study NaCl is considered to be the sole salt in the solution. When constant voltage is applied on the porous electrodes of the CDI cell the effluent concentration drops to a minimum value then it starts to increase again until the feed concentration becomes equal to the effluent concentration; implying that the CDI cell is saturated with salt ions.

In the model proposed by Jande and Kim, the minimum effluent concentration is defined as the "*lowest concentration*" and is given as

$$C_{alowest} = C_f - \frac{\mu}{V_s} y^x (1-y) \tag{1}$$

where C_f is the feed concentration, V_s is the spacer volume, $\mu = \frac{\varepsilon CV}{zF}\left(1 - e^{-\frac{V_s}{\phi R_s C}}\right)$, ε is the Coulombic efficiency, C is the capacitance, V is the applied potential, z is the average valences, F is the Faraday's constant, ϕ is the flow rate, R_s is the resistance, $x = \frac{V_c}{\phi R_s C}$, V_c is the dead volume, and $y = \frac{V_c}{V_c + \phi R_s C}$.

By using genetic algorithm, the CDI operating parameters can be obtained in order to get the lowest effluent concentration close to zero. The reader is requested to refer to Ref. [23] for details on how the CDI parameters, i.e., flow rate, spacer volume, capacitance, dead volume, and resistance, are determined.

B. Reverse Electrodialysis

In this study the model for the RED described by Veerman *et al.*[24] is used. Low salinity stream (LSS) and high salinity stream (HSS) of water passes through the RED of length L and width b (Fig. 3). The LSS has the initial and final concentration of C_L^i and C_L^o, respectively. And for the HSS the initial and outlet concentration is C_H^i and C_H^o, respectively. The width of the LSS compartment and HSS compartment is δ_L and δ_H, respectively. The Cl^- and Na^+ passes through the anion exchange membrane (AEM) and cation exchange membrane (CEM), respectively, with the flux J_{Cl} and J_{Na}.

The model summary is as follows:

$$E_{cell}(x) = \frac{RT}{F}\left[\alpha_{CEM} \ln\left(\frac{\gamma_H^{Na} C_H(x)}{\gamma_L^{Na} C_L(x)}\right) + \alpha_{AEM} \ln\left(\frac{\gamma_H^{Cl} C_H(x)}{\gamma_L^{Cl} C_L(x)}\right)\right] \tag{2}$$

Where R is gas constant, T is temperature, α is membrane selectivity, and γ is activity coefficient.

$$\gamma(x) = \exp\left[\frac{-0.51 v\sqrt{I(x)}}{1 + (A/305)\sqrt{I(x)}}\right] \tag{3}$$

Where v is valence, A is hydrated ion radius in pm (A_{Cl^-} = 300 pm and A_{Na^+} = 450 pm), and $I(x)$ is ion strength of the solution in mol/L and it is given as

$$I(x) = \frac{C(x)}{1000} \tag{4}$$

Note: C should be in mol/m^3. The area resistance in the HSS and LSS compartments is respectively,

$$R_{a,H}(x) = f\frac{\delta_H}{\Lambda_m C_H(x)} \tag{5}$$

$$R_{a,L}(x) = f\frac{\delta_L}{\Lambda_m C_L(x)} \tag{6}$$

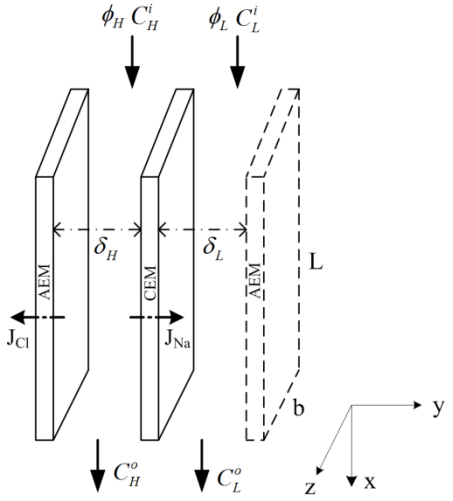

Fig. 3 Undivided RED system

Where Λ_m = 0.013 Sm^2/mol (molar conductivity of NaCl solution) and f = 2 (obstruction factor). The area cell resistance is

$$R_{a,cell}(x) = R_{a,L}(x) + R_{a,H}(x) + R_{AEM} + R_{CEM} \quad (7)$$

Where R_{AEM} and R_{CEM} is AEM and CEM resistance, respectively. For the maximum power the cell resistance should be equal to the load resistance and hence the current density is defined as

$$j(x) = \frac{E_{cell}(x)}{2R_{a,cell}(x)} \quad (8)$$

Salt transport from HSS to LSS is defined as

$$J_{total}(x) = \frac{j(x)}{F} + \frac{2D_{NaCl}}{\delta_m}\left[C_H(x) - C_L(x)\right] \quad (9)$$

Where δ_m is the membrane thickness and D_{NaCl} is the salt diffusion. Since the external resistance and the cell resistance is considered to be the same, then the external power density is given as

$$P_d(x) = \frac{1}{2} j^2(x) R_{a,cell}(x) \quad (10)$$

And the total power developed is

$$P_{total} = b\int_0^L P_d dx \quad (11)$$

The average power density is

$$P_d = \frac{P_{total}}{Lb} \quad (12)$$

And the residence time is

$$t_R = \frac{Lb\delta}{\phi} \quad (13)$$

Where ϕ and δ is the flow rate and compartment spacer, respectively. The volumetric water flux is given as

$$J'_{water} = -\frac{2D_{water}}{\delta_m}\left[C_H(x) - C_L(x)\right]\frac{M_{H_2O}}{\rho_{H_2O}} \quad (14)$$

Where D_{water} is water diffusion constant, M_{H_2O} is molar mass of water, and ρ_{H_2O} is density of water. Transport equations for the salt is given as

$$\frac{d}{dx}C_H(x) = -\frac{b}{\phi_H}J_{total}(x) + C_H(x)\frac{bJ'_{water}}{\phi_H} \quad (15)$$

$$\frac{d}{dx}C_L(x) = \frac{b}{\phi_L}J_{total}(x) - C_L(x)\frac{bJ'_{water}}{\phi_L} \quad (16)$$

The solution of this problem is solved numerically. In this study we are dealing with an undivided case only; and the cell size (with Fumasep Membranes—FAD and FKD) and specification are as that described in section 5.1 of Ref. [24] i.e., cell dimension: 10 cm x 10 cm, $f = 2$, R_{AEM} = 1.63 x 10^{-4} Ωm^2, R_{CEM} = 5.90 x 10^{-4} Ωm^2, $\alpha_{AEM} = \alpha_{AEM} = \alpha = 0.88$, $D_{water} = 1.3\times10^{-9}\,m^2/s$, and $D_{salt} = 0.13\times10^{-10}\,m^2/s$.

C. Hybrid CDI-RED System

The schematic diagram of the hybrid system is shown in Fig. 4. The saline water with the concentration of 15,000 ppm (256 mol/m^3 NaCl) is initially passed through the CDI cell. The outlet of the CDI cell is divided into four streams: fresh water stream, LSS, HSS, and rejected water stream. The LSS and HSS are allowed to pass through the RED cell for electricity generation.

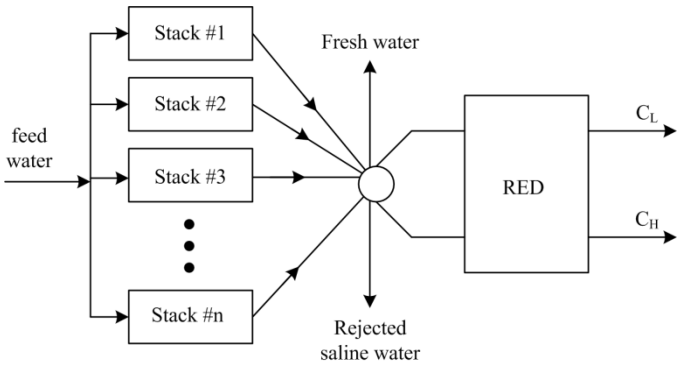

Fig. 4 Schematic diagram of hybrid CDI-RED system

III. Results And Discussion

The values of the CDI cell parameters for the given concentration per electrodes pair are: V = 3.0V, $\phi = 0.3$ mL/s, V_s = V_c = 15 mL, C = 993 F, and $R_s = 0.18\,\Omega$. By using equation (1) found in Ref. [23], the dynamic response of the CDI cell is shown in Fig. 5. The adsorption and desorption time is 126 s and 1074 s, respectively. The average concentration for the LSS is obtained by taking the average of the area under the curve of Fig. 5 between 0 s and 60 s—which is found to be 85 mol/m^3, and for the HSS the average concentration is found between 126 s and 1200 s, which is 289 mol/m^3. Similarly, the average concentration of freshwater is 8.4 mol/m^3 (492 ppm) between 60 s and 126 s; this value is below 500 ppm , and the produced fresh water is thus good for human consumption [25].

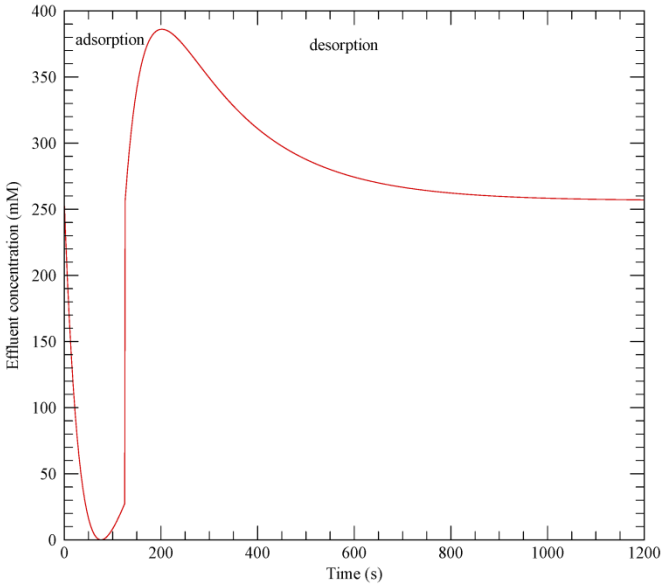

Fig. 5 Dynamic response of the CDI cell

The continuous flow of LSS and HSS is guaranteed by having 21 pairs of electrodes operating at different position (Fig. 6). The red, purple, blue and green color shows that at that duration pair of CDI cell electrodes produces LSS, freshwater,

HSS, and reject water, respectively. The flow rate of LSS and HSS is the same, which is 0.30 mL/s. The salt concentration in LSS increases while in HSS is decreasing in RED system as it is shown in Fig. 7. The salt ions have moved to LSS compartment due to salinity gradient. If the length *L* would have been increased further, the salt concentration in both streams would have changed much more. In Fig. 8 the variation of area cell resistance along the x-direction is presented. The resistance is usually higher in LSS than in HSS. The resistance would become almost constant when the RED cell height increases [24].

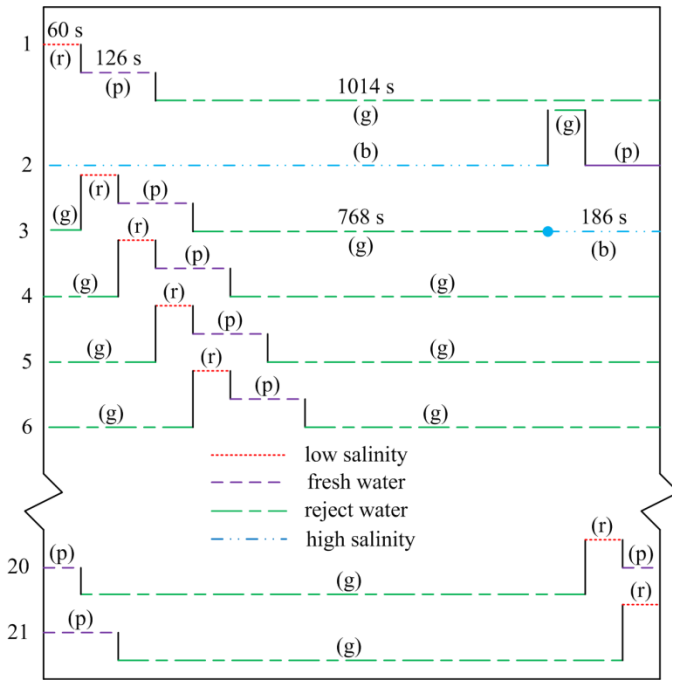

Fig. 6 Switching of the CDI electrode pairs; b: blue, g: green, p: red, and p: purple

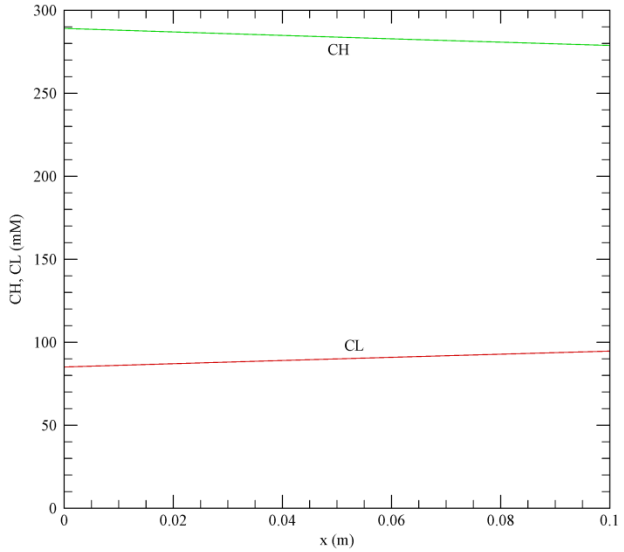

Fig. 7 Variation of HSS and LSS concentration

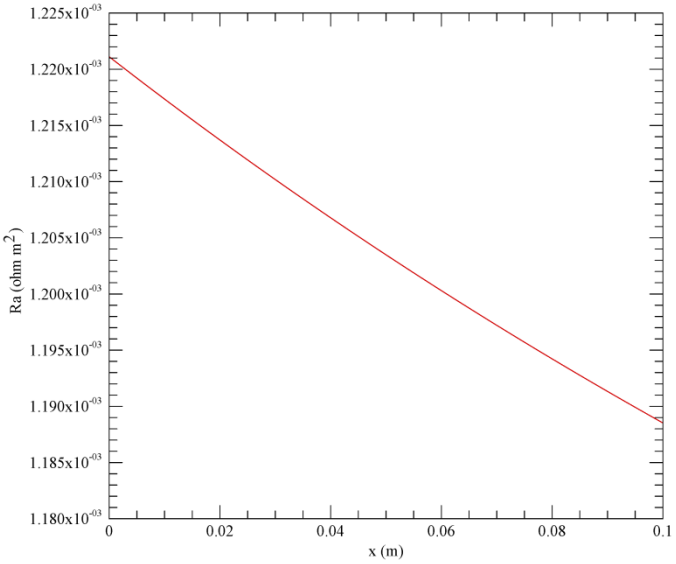

Fig. 8 Cell resistance variations along x-axis

Fig. 9 shows the produced local RED cell voltage. Voltage is decreasing due to the decreasing of salinity gradient along *x*-direction. Electric potential at $x = 0$ is greater because of high salinity gradient between HSS and LSS. At the outlet of RED, open circuit potential has dropped considerably to lower value compared to that of the inlet. The local RED potential can decrease further if the size of the cell becomes much larger than the existing value.

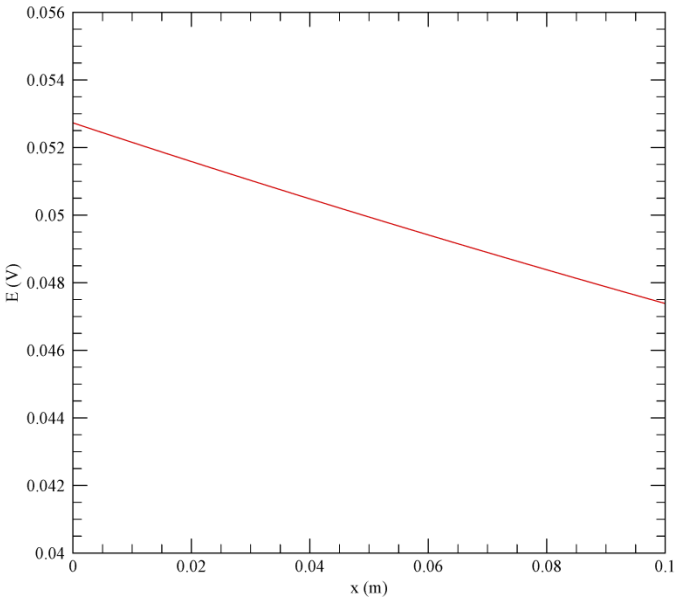

Fig. 9 Local RED cell potential variations along x-direction

The local power density (in W/m^2 membrane surface) of the hybrid CDI-RED system is shown in Fig. 10. In Ref. [24] the power density increases to the maximum and then it drops down, exhibiting a peak value of local power density along *x*-direction. However, in this study we observe a straight line. This phenomena is may be due to salinities of HSS and

LSS—in Ref. [24] seawater and river water were used. More investigation/study is required to explore the fact. The average power density (from Eq. (12)) for the hybrid CDI-RED system is approximately found to be equal to 0.26 W/m^2. This study has an important role in minimizing the concentration of the brine from the CDI cell which would have a negative environmental impact and also in producing green energy.

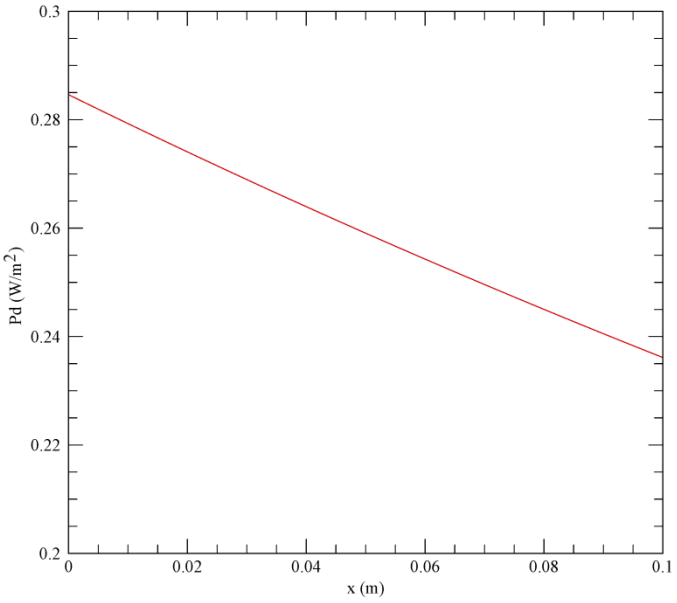

Fig. 10 Power density of the hybrid CDI-RED system

IV. Conclusion

The hybrid CDI-RED system uses a single feed saline water to have freshwater and electric power. A CDI cell charged at constant voltage generates three different streams: fresh water stream, low salt concentrated stream, and high salt concentrated stream. Instead of disposing directly the CDI brine, it can be passed through the RED cell to produce energy. In this study we used 15, 000 ppm as a feed concentration to the hybrid CDI-RED system. More studies can be conducted at higher salinities such as at 40,000 ppm (seawater). Furthermore, extensive studies can be carried out using constant current in CDI cell as in Refs. [11, 26, 27] so that the two hybrid systems, i.e., constant voltage driven CDI-RED and constant current driven CDI-RED can be compared in terms of performance. The overall capital cost and operational cost can be investigated to see the feasibility of commercializing the concept.

Acknowledgment

This work was supported by the National Research Foundation of Korea (NRF) with grant number NRF-2011-0017220.

References

[1] L.F. Greenlee, D.F. Lawler, B.D. Freeman, B. Marrot, P. Moulin, Reverse osmosis desalination: Water sources, technology, and today's challenges, Water Res., 43 (2009) 2317-2348. http://dx.doi.org/10.1016/j.watres.2009.03.010

[2] S. Phuntsho, S. Hong, M. Elimelech, H.K. Shon, Forward osmosis desalination of brackish groundwater: Meeting water quality requirements for fertigation by integrating nanofiltration, J. Membr. Sci., 436 (2013) 1-15. http://dx.doi.org/10.1016/j.memsci.2013.02.022

[3] A.A.A. Attia, New proposed system for freeze water desalination using auto reversed R-22 vapor compression heat pump, Desalination, 254 (2010) 179-184. http://dx.doi.org/10.1016/j.desal.2009.11.030

[4] A. Al-Karaghouli, L.L. Kazmerski, Energy consumption and water production cost of conventional and renewable-energy-powered desalination processes, Renewable Sustainable Energy Rev., 24 (2013) 343-356. http://dx.doi.org/10.1016/j.rser.2012.12.064

[5] M. Khayet, T. Matsuura, Membrane distillation: principles and applications, Access Online via Elsevier, 2011.

[6] R. Fujioka, L.P. Wang, G. Dodbiba, T. Fujita, Application of progressive freeze-concentration for desalination, Desalination, 319 (2013) 33-37. http://dx.doi.org/10.1016/j.desal.2013.04.005

[7] H. Ni, R.C. Amme, Y. Jin, Desalination by electret technology, Desalination, 174 (2005) 237-245. http://dx.doi.org/10.1016/j.desal.2004.10.002

[8] J. Kuipers, S. Porada, Wireless Desalination Using Inductively Powered Porous Carbon Electrodes, Sep. Purif. Technol., (2013).

[9] J.C. Farmer, D.V. Fix, G.V. Mack, R.W. Pekala, J.F. Poco, Capacitive deionization of NaCl and NaNO3 solutions with carbon aerogel electrodes, J. Electrochem. Soc., 143 (1996) 159-169. http://dx.doi.org/10.1149/1.1836402

[10] M.A. Anderson, A.L. Cudero, J. Palma, Capacitive deionization as an electrochemical means of saving energy and delivering clean water. Comparison to present desalination practices: Will it compete?, Electrochim. Acta, 55 (2010) 3845-3856. http://dx.doi.org/10.1016/j.electacta.2010.02.012

[11] Y.A.C. Jande, W.S. Kim, Desalination using capacitive deionization at constant current, Desalination, 329 (2013) 29-34. http://dx.doi.org/10.1016/j.desal.2013.08.023

[12] S.-i. Jeon, H.-r. Park, J.-g. Yeo, S. Yang, C.H. Cho, M.H. Han, D.K. Kim, Desalination via a new membrane capacitive deionization process utilizing flow-electrodes, Energy Environ. Sci., 6 (2013) 1471. http://dx.doi.org/10.1039/c3ee24443a

[13] Y.-J. Kim, J.-H. Kim, J.-H. Choi, Selective removal of nitrate ions by controlling the applied current in membrane capacitive deionization (MCDI), J. Membr. Sci., 429 (2013) 52-57. http://dx.doi.org/10.1016/j.memsci.2012.11.064

[14] Y.J. Kim, J.H. Choi, Selective removal of nitrate ion using a novel composite carbon electrode in capacitive deionization, Water Res., 46 (2012) 6033-6039. http://dx.doi.org/10.1016/j.watres.2012.08.031

[15] S. Porada, R. Zhao, A. van der Wal, V. Presser, P.M. Biesheuvel, Review on the science and technology of water desalination by capacitive deionization, Prog. Mater Sci., (2013). http://dx.doi.org/10.1016/j.pmatsci.2013.03.005

[16] H. Rodhe, A Comparison of the Contribution of Various Gases to the Greenhouse Effect, Science, 248 (1990) 1217-1219. http://dx.doi.org/10.1126/science.248.4960.1217

[17] G. Marland, T.A. Boden, R.J. Andres, A. Brenkert, C. Johnston, Global, regional, and national fossil fuel CO2 emissions, Trends: A compendium of data on global change, (2003) 34-43.

[18] D.A. Vermaas, J. Veerman, N.Y. Yip, M. Elimelech, M. Saakes, K. Nijmeijer, High Efficiency in Energy Generation from Salinity Gradients with Reverse Electrodialysis, ACS Sustainable Chemistry & Engineering, (2013) 130823083206009.

[19] J. Veerman, M. Saakes, S.J. Metz, G.J. Harmsen, Electrical Power from Sea and River Water by Reverse Electrodialysis: A First Step from the Laboratory to a Real Power Plant, Environ. Sci. Technol., 44 (2010) 9207–9212. http://dx.doi.org/10.1021/es1009345

[20] E. Brauns, Salinity gradient power by reverse electrodialysis: effect of model parameters on electrical power output, Desalination, 237 (2009) 378–391. http://dx.doi.org/10.1016/j.desal.2008.10.003

[21] E. Bram, Combination of a desalination plant and a salinity gradient power reverse electrodialysis plant and use thereof, in: U.S. Patents (Ed.), Vlaamse lflstelhng Voor Technologlsch onderzoek (VITO), M01 (BE), USA, 2008.

[22] W. Li, W.B. Krantz, E.R. Cornelissen, J.W. Post, A.R.D. Verliefde, C.Y. Tang, A novel hybrid process of reverse electrodialysis and reverse osmosis for low energy seawater desalination and brine management, Appl. Energy, 104 (2013) 592-602. http://dx.doi.org/10.1016/j.apenergy.2012.11.064

[23] Y.A.C. Jande, W.S. Kim, Predicting the lowest effluent concentration in capacitive deionization, Sep. Purif. Technol., 115 (2013) 224-230. http://dx.doi.org/10.1016/j.seppur.2013.05.022

[24] J. Veerman, M. Saakes, S.J. Metz, G.J. Harmsen, Reverse electrodialysis: A validated process model for design and optimization, Chem. Eng. J. (Lausanne), 166 (2011) 256-268. http://dx.doi.org/10.1016/j.cej.2010.10.071

[25] WHO, Guidelines for Drinking-water Quality Fourth Edition, World Healthy Organization, Malta, 2011.

[26] P. Dlugolecki, A. van der Wal, Energy recovery in membrane capacitive deionization, Environ. Sci. Technol., 47 (2013) 4904-4910. http://dx.doi.org/10.1021/es3053202

[27] R. Zhao, P.M. Biesheuvel, A. van der Wal, Energy consumption and constant current operation in membrane capacitive deionization, Energy Environ. Sci., 5 (2012) 9520. http://dx.doi.org/10.1039/c2ee21737f